EPJ Web of Conferences **60**, 13005 (2013)
DOI: 10.1051/epjconf/20136013005

First LHCb results from proton-lead collisions at $\sqrt{s_{\rm NN}}$ = 5 TeV

Burkhard Schmidt[1,a], on behalf of the LHCb collaboration.

[1] *CERN, Geneva, Switzerland*

Abstract. The LHCb collaboration studied the production of J/ψ mesons in proton-lead collisions at a proton-nucleon centre-of-mass energy $\sqrt{s_{\rm NN}}$ = 5 TeV. The measurement has been used to determine the nuclear modification factor and to compare the result with theoretical predictions. The analysis is based on a data sample corresponding to an integrated luminosity of about 1 nb^{-1}.

1 Introduction

The study of proton-nucleus collisions is important for heavy ion physics, as it provides essential input to the understanding of nucleus-nucleus collisions. The program carried out at the LHC on proton-lead collisions with an energy per nucleon in the multi-TeV domain, initiated with a short pilot run in September 2012 and continued with a longer run in 2013, has motivated many theoretical studies [1–9]. Previous experiments, performed at lower energy per nucleon, have shown that both quarkonium [10] and light hadron [11, 12] production at large rapidity y is highly suppressed in proton-lead collisions with respect to proton-proton collisions. In addition it was found that forward and backward J/ψ production are different[10, 13], where "forward" and "backward" are defined relative to the direction of the proton beam. This indicates that the nuclear modification factor

$$R_{pA}(y,\sqrt{s_{\rm NN}}) = \frac{1}{A}\frac{\frac{{\rm d}\sigma_{pA}}{{\rm d}y}(y,\sqrt{s_{\rm NN}})}{\frac{{\rm d}\sigma_{pp}}{{\rm d}y}(y,\sqrt{s_{\rm NN}})} \qquad (1)$$

strongly depends on y, where A is the atomic mass number of the nucleus, y is defined as the rapidity with respect to the proton direction in the proton-nucleon centre-of-mass frame, and $\sqrt{s_{\rm NN}}$ is the centre-of-mass energy of the proton-nucleon system.

Despite its asymmetric layout, the LHCb experiment [14] allows measurement of R_{pA} for both positive and negative rapidities. In proton-proton (pp) collisions the J/ψ production cross-section, ${\rm d}\sigma_{pp}/{\rm d}y$, is forward-backward symmetric and is determined in the region $2.0 < y < 4.5$. The production cross-section in proton-lead collisions ${\rm d}\sigma_{pA}/{\rm d}y$ for forward rapidities is measured with the proton beam moving from the interaction point toward the detector (pA collisions in the following). Data collected with the inverted beam directions (Ap in the following) allow to measure backward production. The measurement of the nuclear modification factor as a function of rapidity will be helpful for the interpretation of cold nuclear effects using different models.

Data were collected with a proton beam energy of 4 TeV and a lead beam energy of 1.58 TeV per nucleon, resulting in a centre-of-mass energy of the proton-nucleon system of 5 TeV. Since the energy of the proton beam is significantly larger than that of the nucleon in the lead beam, the proton-nucleon centre-of-mass system has a rapidity in the laboratory frame of +0.47 for pA and −0.47 for Ap collisions. This boost results in a shift of the rapidity coverage in the proton-nucleon centre-of-mass system, ranging from about 1.5 to 4.0 for pA collisions and from −5.0 to −2.5 for Ap collisions. Throughout these proceedings y always indicates the rapidity in the proton-nucleon centre-of-mass system, unless otherwise specified.

In this analysis the two-dimensional dependence on y and on the transverse momentum $p_{\rm T}$ of the J/ψ production cross-section is measured in pA collisions. Due to limited sample size, only the one-dimensional dependence on either y or $p_{\rm T}$ is measured in Ap collisions.

The analysis is based on data samples corresponding to integrated luminosities of 0.75 nb^{-1} of pA and 0.30 nb^{-1} of Ap collisions. The luminosities are determined from online measurements with an estimated uncertainty of 5%.

2 Determination of the J/ψ production cross-section

The strategy for the J/ψ production measurement is based on that described in Refs. [15–17]. The J/ψ candidates are reconstructed and selected using the $J/\psi \to \mu^+\mu^-$ channel. Events with at least one primary vertex are selected, where the primary vertex is reconstructed from at least five tracks in the vertex locator (VELO) of LHCb. The J/ψ candidates are formed from tracks with opposite sign charges. The tracks should be identified as muons by the muon detector, and the difference between the logarithms of the likelihoods for the muon and the pion hypotheses should

[a] e-mail: Burkhard.Schmidt@cern.ch

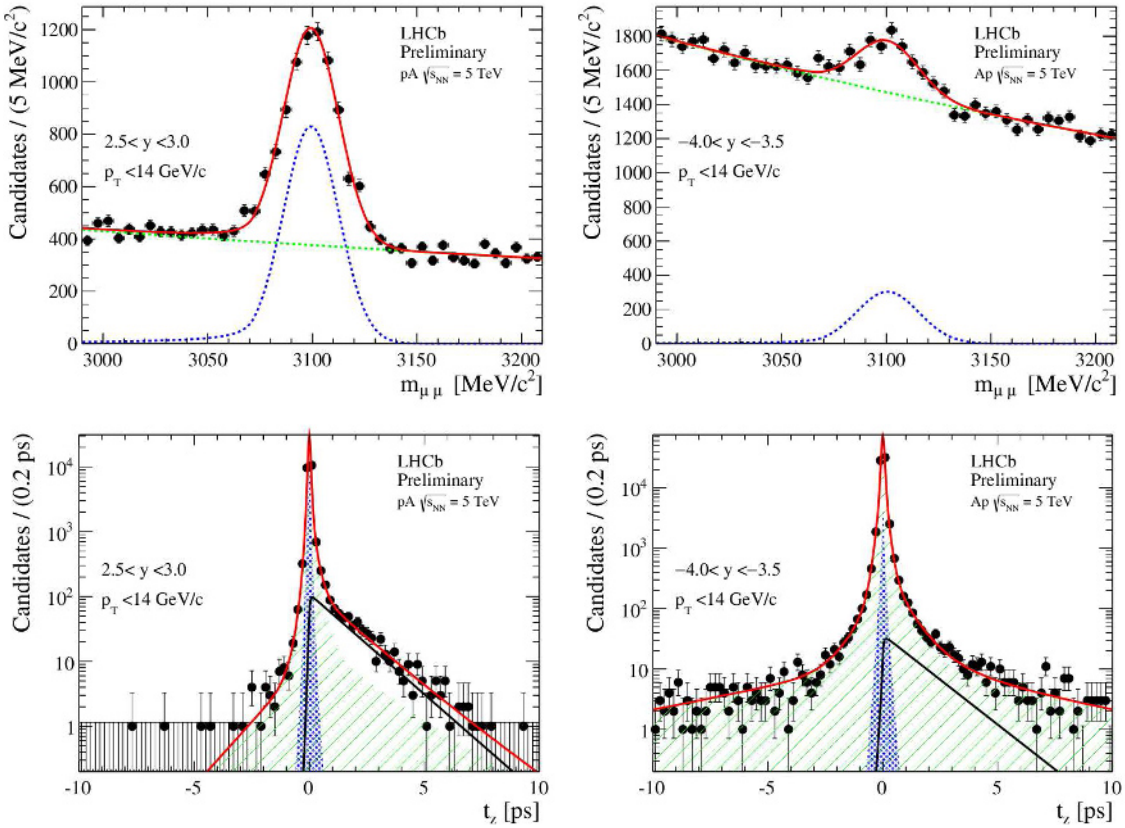

Figure 1. Examples for projections of the fit results onto (top) invariant dimuon mass and (bottom) t_z in pA (left, $2.5 < y < 3.0$) and Ap (right, $-4.0 < y < -3.5$). The data are integrated over transverse momentum, $p_T < 14$ GeV/c. For the mass projection, the total fitted function is shown (red solid line) together with the signal distribution including J/ψ from b-hadrons (blue dotted line) and background (green dotted line). For the t_z projection the total fitted function is shown by the solid red line, the background component is shown as the green hatched area, the prompt signal component by the blue area, the J/ψ from b-hadrons by the solid black line.

be greater than one. A p_T above 0.7 GeV/c and a good track fit quality (χ^2/ndf < 4) are required for each track. The two muons are required to originate from a common vertex with a χ^2-probability larger than 0.5%. The candidates are kept if the invariant mass falls in a mass window of $\pm 120\,\mathrm{MeV}/c^2$ around the known J/ψ mass [18].

The determination of the double-differential production cross-section requires knowledge of the numbers of prompt J/ψ, J/ψ from b-hadron and background decays in bins of the kinematic variables y and p_T. This is done by performing a simultaneous fit to the distributions of the dimuon invariant mass and the pseudo-proper time t_z in each kinematic bin. The pseudo-proper time of the J/ψ is defined as

$$t_z = \frac{(z_{J/\psi} - z_{PV}) \times M_{J/\psi}}{p_z}, \qquad (2)$$

where $z_{J/\psi}$ is the z position of the J/ψ decay vertex, z_{PV} that of the primary vertex refitted after removing the two muon tracks from the J/ψ candidate, p_z the measured J/ψ momentum along the beam axis z, and $M_{J/\psi}$ the known J/ψ mass. The pseudo-proper time t_z is a Lorentz invariant variable which allows to separate prompt particles from J/ψ mesons created in decays of b-hadrons.

The signal dimuon invariant mass distribution in each p_T and y bin is modelled by a Crystal Ball (CB) function [19], while the combinatorial background is described by an exponential function. The t_z signal distribution is described by the sum of a delta function at $t_z = 0$ for the prompt J/ψ and an exponential decay function for the J/ψ component from b, convolved with a resolution function modelled by a double-Gaussian function. The t_z background distribution is modelled with an empirical function based on the shape of the t_z distribution that is observed in the J/ψ mass sidebands. All the parameters of the background function are determined from sidebands independently in each bin of p_T and y. These parameters are then fixed in the final simultaneous fits to the distributions of invariant mass and pseudo-proper time. The total fit function is the sum of the products of the mass and t_z fit functions for the signal and background components. Figure 1 shows projections of the fit on mass and t_z for a typical bin for pA data. The resolutions of the dimuon invariant mass in pA and Ap collisions are consistent with each other, about 15 MeV, and are both consistent with that in pp collisions.

Based on the fit result, for each of the two components, namely prompt J/ψ and J/ψ from b, a signal weight factor w_i for the i^{th} candidate is obtained with the *sPlot* technique [20], using the dimuon invariant mass and t_z as separating variables. The sum of w_i over all candidates in a given p_T and y bin gives the number of signal candidates in the bin, n_{sig}, while the sum of w_i^2 gives the vari-

ance of $n_{\rm sig}$. For the event-by-event efficiency correction the sum of w_i/ϵ_i over a given bin leads to the efficiency corrected signal yield $N^{\rm cor}$ in the bin. The efficiency ϵ_i depends on $p_{\rm T}$ and y and includes the geometrical acceptance, trigger and reconstruction efficiencies. The acceptance and reconstruction efficiencies are estimated from the simulated samples mentioned above, while the trigger efficiency is obtained from the data by exploiting a sample of J/ψ events that would still be triggered if the J/ψ candidates were removed.

The double differential cross-section for J/ψ production in a given $(p_{\rm T}, y)$ bin is defined as

$$\frac{{\rm d}^2\sigma}{{\rm d}p_{\rm T}{\rm d}y} = \frac{N^{\rm cor}(J/\psi \to \mu^+\mu^-)}{\mathcal{L} \times \mathcal{B}(J/\psi \to \mu^+\mu^-) \times \Delta p_{\rm T} \times \Delta y}, \quad (3)$$

where $N^{\rm cor}(J/\psi \to \mu^+\mu^-)$ is the efficiency corrected number of $J/\psi \to \mu^+\mu^-$ signal candidates in the given bin. In the denominator, $\mathcal{L}$ is the integrated luminosity, $\mathcal{B}(J/\psi \to \mu^+\mu^-) = (5.93 \pm 0.06)\%$ [18] the branching fraction of the $J/\psi \to \mu^+\mu^-$ decay, and $\Delta p_{\rm T}$ and Δy the widths of the $p_{\rm T}$ and y bins. The transverse momentum range $p_{\rm T} < 14$ GeV/c is divided into 8 bins, with $\Delta p_{\rm T} = 1$ GeV/c for $p_{\rm T} < 7$ GeV/c and $\Delta p_{\rm T} = 7$ GeV/c for $7 < p_{\rm T} < 14$ GeV/c. The rapidity bin width is $\Delta y = 0.5$.

3 Systematic uncertainties

The different contributions to the systematic uncertainties affecting the cross-section measurement are discussed in the following and summarised in Table 1. The influence of the fit function used to describe the shape of the dimuon invariant mass distribution is estimated by fitting the invariant mass distribution with the sum of two Crystal Ball functions. The total relative difference of 1.8% in the signal yield is taken as systematic uncertainty. The uncertainty of the luminosity determination is estimated to be 5% according to earlier studies [21]. The uncertainty due to reconstruction efficiency of the muon tracks is estimated using a data-driven tag-and-probe approach [22] based on partially reconstructed J/ψ decays. Taking into account the effect of the track multiplicity difference between proton-ion and proton-proton data, this results in an uncertainty of 1.5%. The uncertainties related to the radiative tail, vertexing, track quality and muon identification are taken from Refs. [15–17], but have been increased conservatively by 30%, leading to an overall uncertainty of 3.5%. The same has been done for the uncertainty due to the t_z fit procedure, which only affects the component of J/ψ from b. An uncertainty of 5% has been conservatively assigned. No systematic uncertainty has been assigned to the effect of polarisation in this analysis.

Differences in the $p_{\rm T}$ and y spectra between the data and MC can effect the result because of the finite size of the bins. To estimate the size of this effect the total efficiency has been checked by doubling the number of bins in $p_{\rm T}$ and rapidity. The relative difference with respect to the nominal binning, which varies between 0.1% and 14% depending on the bin, is taken as systematic uncertainty.

Table 1. Relative systematic uncertainties on the differential production cross-section.

Source	Syst. uncertainty (%)
Correlated between bins	
Mass fits	1.8
Tracking efficiency	1.5
$\mathcal{B}(J/\psi \to \mu^+\mu^-)$	1.0
Luminosity	5.0
Vertexing, track quality, etc.	3.5
Uncorrelated between bins	
t_z fit (*only for J/ψ from b)*	5.0
Binning	0.1 to 14

4 Results

The differential cross-sections for prompt J/ψ production and J/ψ from b in pA and Ap collisions as a function of $p_{\rm T}$ and y are displayed in Fig. 2.

The integrated cross-sections in the range of $p_{\rm T} < 14$ GeV/c and $1.5 < y < 4.0$ for prompt J/ψ production and J/ψ from b in pA data are

$$\sigma_{\rm pA}(\text{prompt } J/\psi) = 1028.2 \pm 13.6\,(\text{stat.}) \pm 88.6\,(\text{syst.})\ \mu\text{b},$$
$$\sigma_{\rm pA}(J/\psi \text{ from } b) = 150.1 \pm 4.2\,(\text{stat.}) \pm 12.6\,(\text{syst.})\ \mu\text{b}.$$

The integrated cross-sections in the range of $p_{\rm T} < 14$ GeV/c and $-5.0 < y < -2.5$ for the prompt J/ψ production and J/ψ from b in Ap data are

$$\sigma_{\rm Ap}(\text{prompt } J/\psi) = 1141.9 \pm 49.8\,(\text{stat.}) \pm 98.4\,(\text{syst.})\ \mu\text{b},$$
$$\sigma_{\rm Ap}(J/\psi \text{ from } b) = 119.7 \pm 8.3\,(\text{stat.}) \pm 10.0\,(\text{syst.})\ \mu\text{b}.$$

The simultaneous fits to the invariant mass and t_z distributions in pA and Ap collisions give the fraction of J/ψ from b as a function of $p_{\rm T}$ or y. These results are consistent with those measured in pp collisions with centre-of-mass energies of 2.76, 7 and 8 TeV [15–17].

The integrated cross-sections for J/ψ production in pA, Ap and pp collisions can be compared in the common rapidity range of the proton-nucleon system, $2.5 < |y| < 4.0$. After integration over this range and the full transverse momentum range, the cross-section of prompt J/ψ production in Ap collisions is approximately 50% higher than that in pA collisions. This result indicates that J/ψ production is less suppressed in the backward region of proton-nucleus collisions. The cross-sections of prompt J/ψ production in pA collisions are about 170 times larger than those in pp collisions at 2.76 TeV and about 80 times larger than those in pp collisions at 7 TeV and 8 TeV. For Ap collisions, these numbers are roughly 260 and 130, respectively.

Figure 3 (left) shows the cross-sections for prompt J/ψ production scaled by a factor of $1/A$ in the common rapidity range $2.5 < |y| < 4.0$ of the proton-nucleon system at different centre-of-mass energies. Within the kinematic range of this analysis, the J/ψ production cross-section in pp collisions at 5 TeV can be obtained by linear interpolation from previous LHCb measurements at 2.76, 7 and 8 TeV .

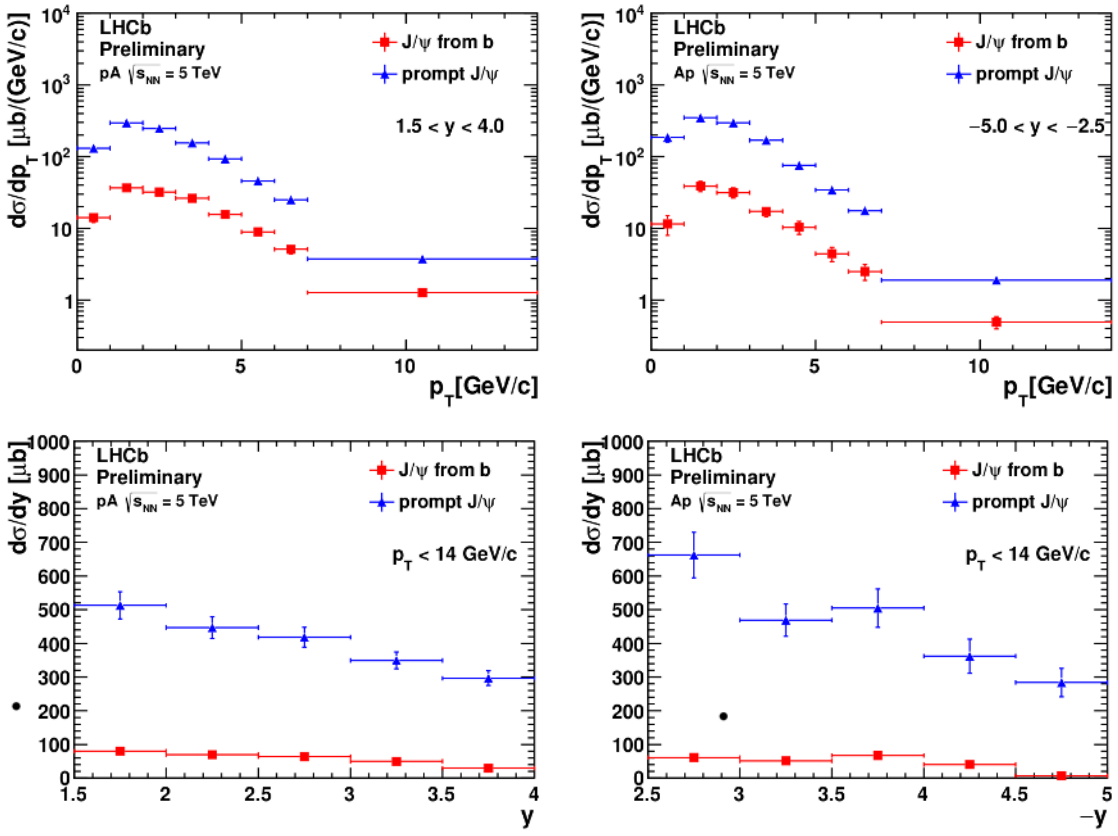

Figure 2. Differential cross-sections for prompt J/ψ mesons and J/ψ from b-hadrons as function of p_{T} (top) and rapidity y (bottom) in pA (left, $1.5 < y < 4.0$) and Ap (right, $-5.0 < y < -2.5$) collisions.

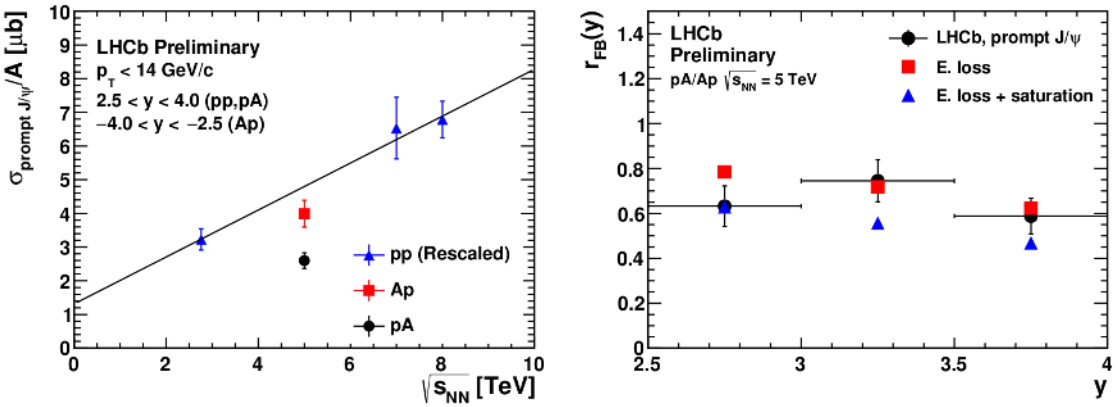

Figure 3. Left: Cross-sections for prompt J/ψ production scaled by a factor of $1/A$ and integrated over the common rapidity range of the proton-nucleon system, $2.5 < y < 4.0$ for pp and pA collisions, and $-4.0 < y < -2.5$ for Ap collisions. The blue triangles stand for the cross-sections at 2.76, 7 and 8 TeV in the same kinematic region. The black line is a linear fit to these three points. The red square and black dots below the line are the scaled cross-sections in Ap and pA collisions.
Right: Forward-backward ratio r_{FB} as a function of rapidity in the range of 2.5 to 4.0 of the proton-nucleon centre-of-mass system. The black dots indicate the data, while the blue triangles and red squares are theoretical predictions, taking into account the effects of parton energy loss in cold nuclear matter with and without saturation effects [2].

The ratio of attenuation factors in the forward (pA) and backward (Ap) regions, $r_{\mathrm{FB}}(y) \equiv R_{pA}(y)/R_{Ap}(-y)$, defines the forward-backward production asymmetry. A deviation from unity indicates nuclear effects in proton-nucleus collisions. Figure 3 (right) shows the ratio r_{FB} as a function of y in the common rapidity range of the proton-nucleon system, together with the theoretical predictions of Ref. [2]. The dots indicate the measurements from data, while the triangles and squares are theoretical predictions taking into account the effects of parton energy loss [23, 24] in cold nuclear matter with and without saturation effects [25]. The data are consistent with both predictions, *i.e.* the cur-

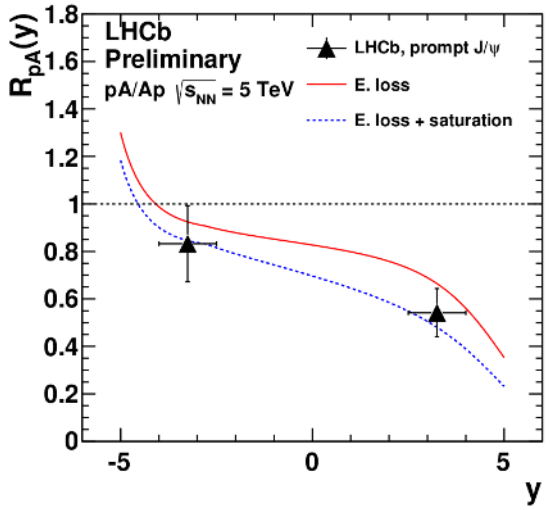

Figure 4. Modification factor R_{pA} determined in data compared to theoretical predictions [2]. The black triangles are LHCb measurements, the red solid line is the theoretical prediction based on parton energy loss effects, the blue dashed line takes additional saturation effects into account.

rent precision is not sufficient to evaluate the importance of saturation effects.

Using the prompt J/ψ production cross-section in pp collisions at 5 TeV, obtained by linear interpolation from previous LHCb measurements, as shown in Fig. 3, the nuclear modification factor, R_{pA}, can be determined. Figure 4 shows R_{pA} in the range of $-4.0 < y < -2.5$ and $2.5 < y < 4.0$, together with the comparison to the theoretical predictions of Ref. [2]. The interpolation error for the J/ψ production cross-section in pp collisions at 5 TeV is taken into account. Within the sizeable uncertainties of the current measurements, the result agrees with the theoretical predictions.

5 Conclusion

The production of J/ψ mesons is studied in proton-lead collisions with the LHCb detector at a proton-nucleon centre-of-mass energy $\sqrt{s_{NN}} = 5$ TeV in the transverse momentum range of $p_T < 14$ GeV/c and rapidity range $1.5 < y < 4.0$ (pA) and $-5.0 < y < -2.5$ (Ap). The nuclear attenuation factor R_{pA} is determined, where the cross-section of J/ψ production in pp collisions at 5 TeV is interpolated from previous LHCb measurements at 2.76, 7 and 8 TeV. The forward-backward asymmetry ratio r_{FB} is determined as a function of rapidity. These preliminary results show good agreement with the theoretical predictions in Ref. [2]. An update of the analysis is presently ongoing, using the full data-set of proton-lead collisions collected by LHCb in 2013 of about 1.6 nb^{-1} and improved muon identification criteria to suppress the huge combinatorial background in Ap collisions, as shown in the invariant dimuon mass distribution of Fig. 1.

References

[1] J. Albacete, N. Armesto, R. Baier, G. Barnafoldi, J. Barrette et al., Int. J. Mod. Phys. **E22**, 1330007 (2013), 1301.3395

[2] F. Arleo, S. Peigne, JHEP **03**, 122 (2013), 1212.0434

[3] A. Adeluyi, T. Nguyen, Phys.Rev. **C87**, 027901 (2013), 1302.4288

[4] G.A. Chirilli, B.W. Xiao, F. Yuan, Phys.Rev. **D86**, 054005 (2012), 1203.6139

[5] D. Kharzeev, E. Levin, K. Tuchin (2012), 1205.1554

[6] J. Lansberg (2012), 1209.0331

[7] G.A. Chirilli, Int.J.Mod.Phys.Conf.Ser. **20**, 200 (2012), 1209.1614

[8] A. Adeluyi, T. Nguyen (2012), 1210.3327

[9] F. Arleo, R. Kolevatov, S. Peigne, M. Rustamova (2013), 1304.0901

[10] M. Leitch et al. (FNAL E866/NuSea collaboration), Phys.Rev.Lett. **84**, 3256 (2000), nucl-ex/9909007

[11] I. Arsene et al. (BRAHMS collaboration), Phys.Rev.Lett. **93**, 242303 (2004), nucl-ex/0403005

[12] S. Adler et al. (PHENIX collaboration), Phys.Rev.Lett. **94**, 082302 (2005), nucl-ex/0411054

[13] A. Adare et al. (PHENIX collaboration), Phys.Rev.Lett. **107**, 142301 (2011), 1010.1246

[14] A.A. Alves Jr. et al. (LHCb collaboration), JINST **3**, S08005 (2008)

[15] R. Aaij et al. (LHCb collaboration), Eur. Phys. J. **C71**, 1645 (2011), 1103.0423

[16] R. Aaij et al. (LHCb collaboration), JHEP **02**, 041 (2013), 1212.1045

[17] R. Aaij et al. (LHCb collaboration) (2013), submitted to JHEP, 1304.6977

[18] J. Beringer et al. (Particle Data Group), Phys. Rev. **D86**, 010001 (2012)

[19] T. Skwarnicki, Ph.D. thesis, Institute of Nuclear Physics, Krakow (1986), DESY-F31-86-02

[20] M. Pivk, F.R. Le Diberder, Nucl.Instrum.Meth. **A555**, 356 (2005), physics/0402083

[21] LHCb collaboration, *First analysis of the pPb pilot run data with LHCb*, LHCb-CONF-2012-034

[22] A. Jaeger et al. *Measurement of the track finding efficiency*, LHCb-PUB-2011-025

[23] R. Baier, Y.L. Dokshitzer, A.H. Mueller, S. Peigne, D. Schiff, Nucl.Phys. **B483**, 291 (1997), hep-ph/9607355

[24] B. Zakharov, JETP Lett. **65**, 615 (1997), hep-ph/9704255

[25] F. Gelis, T. Lappi, R. Venugopalan, Int.J.Mod.Phys. **E16**, 2595 (2007), 0708.0047